JEE Journal of Ecological Engineering

Journal of Ecological Engineering 2024, 25(8), 1–9
https://doi.org/10.12911/22998993/189230
ISSN 2299–8993, License CC-BY 4.0

Received: 2024.05.13
Accepted: 2024.06.17
Published: 2024.07.01

Improving the Efficiency of Water Purification from Heavy Metals using the Electric Spark Method

Sergei Petrichenko[1], Antonina Malushevskaya[1], Artem Ivanov[1], Olena Mitryasova[2*], Ivan Salamon[3]

[1] Institute of Pulse Processes and Technologies of NAS of Ukraine, Av. Bogoyavlenskyi, 43a, Mykolaiv, 54018, Ukraine
[2] Petro Mohyla Black Sea National University, 68 Desantnykiv, 10, Mykolaiv, 54003, Ukraine
[3] University of Presov, Slovakia, ul. 17. Novembra 15, Prešov, 08001, Slovakia
* Corresponding author's e-mail: lesya.solis28@gmail.com

ABSTRACT

Ways to increase the efficiency of the electric spark method of wastewater purification from heavy metal ions by increasing the stability of discharges and reducing energy losses are shown. General regularities of changes in the electrical characteristics of a multi-spark underwater discharge distributed in a layer of a mixture of iron and aluminum granules from the parameters of the discharge circuit have been revealed. The dependencies of the power amplitudes of electric spark discharges in a layer of metal granules on time under conditions of different combinations of inductance and capacitance of the discharge circuit are formalized, the regularities of energy input into working reactors to regulate the conditions and efficiency of purification are considered.

Keywords: water quality, water purification, heavy metals, electric spark method, energy efficiency of electric spark discharge.

INTRODUCTION

Water security is one of the priorities of national and European policies to ensure the goals of sustainable development. Ecologically destructive models of development in many countries of the world have led to the degradation of water resources, which is reflected in their volume and quality (Mitryasova et al., 2016; Mitryasova and Pohrebennyk, 2017). The need arises to ensure the optimal use of water, protection of freshwater resources, monitoring of water resources, the search for new technologies and methods of wastewater treatment, the investigation of the quality of drinking water.

Pollution of the aquatic environment with heavy metal ions is dangerous for the entire biosphere, and is also a consequence of wasteful use of resources. Industrial wastewater from many chemical, textile, machine-building, electrotechnical plants, non-ferrous metallurgy enterprises and other industries is polluted to varying degrees with non-ferrous and heavy metal salts. Most often, they are contaminated with salts of zinc, cadmium, copper, chromium, nickel, mercury, iron, less often they contain cobalt and manganese. Wastewater rarely contains only one type of cations, but rather a mixture of several salts of mineral acids. The problem of complex wastewater treatment from heavy metal ions exists in many industries. It is especially relevant now, when the global community is on the brink of an environmental crisis. The research and development of simple and technological methods for purifying polluted water from industrial enterprises from heavy metal ions are of undoubted interest.

Electric spark discharge between conductive granules is an effective tool for the purification of industrial effluents from electroplating production and other polluted water from heavy metal ions. Technological methods based on this type of discharge are also called by various groups of researchers and developers electropulse cleaning of electroplating and waste disposal, electroerosive

dispersion of conductive granules, and electric pulse method of complex processing of materials.

The technical implementation of electric spark methods is as follows. A charged capacitor battery is periodically switched to the space between two conductive electrodes, which are metal planes or coaxially arranged hollow cylinders. The space between the electrodes is freely filled with electrically conductive granules, the granules are immersed in a weakly conductive liquid. With each switching, local electrical discharges (plasma erosion regions) occur on the many contacting areas of the granule surfaces. A set of plasma erosion regions forms several chains that close the entire gap between the electrodes.

Electric spark discharges at the contacts between granules in the liquid, the mechanisms of spark erosion dispersion of the granule material, and the accompanying electric spark purification of water containing metal ions have been actively studied since the beginning of the 21st century, up to the present time (Berkowitz et al., 2003; Carrey et al., 2002; Zakharchenko et al., 2002; Lobanova et al., 2015; Malyushevskaya et al., 2023). A large number of studies in this area are narrowly focused and relate to the solution of specific technological tasks and scientific problems (Béjar et al., 2006; Milligan et al., 2013; Petrov et al., 2020; Wang et al., 2022; Zakharchenko et al., 2018).

If a mixture of granules of different metals is used in the process of electric spark treatment (combined metal loading), for example, a mixture of iron and aluminum, then this significantly expands the possibilities of electric spark purification of water from ions of various heavy metals. By pumping contaminated water from electroplating plants through a layer of iron and aluminum granules, between which electric spark discharges occurred, the authors [9] achieved comprehensive water purification from heavy metal ions (Ni^{2+}, Zn^{2+}, Cr^{6+}+Cr^{3+}, Cu^{2+}, Fe(Σ) to their residual content less than provided for by the current standards for maximum permissible concentrations. However, in the course of the work, the authors noted that the stability of electric spark discharges and their reproducibility is the "weak" point of the method.

To date, there have been no generalized results on the conditions of stabilization of electrical modes of water purification from heavy metal ions using electric spark discharges using a mixture of metal granules of different compositions. The dependencies of the power amplitudes of electric spark discharges and the regularities of energy input into the interelectrode gap on the parameters of the discharge circuit have not been investigated. Such regularities determine the temporal and spatial distribution of plasma erosion areas in the granule layer, temperature and other conditions. In the final analysis, the efficiency of water purification from heavy metal ions depends on the stability of the volume distribution of a multi-spark underwater discharge.

Thus, the purpose of this work was to determine the conditions that allow the electro-spark discharge between conductive granules in a liquid to be stabilized. For this purpose, it was necessary to identify the general patterns of changes in the electrical and energy characteristics of electric spark discharges in a layer of metal granules depending on the parameters of the discharge circuit.

MATERIALS AND METHODS

Electric spark discharges between metal loading granules were implemented using a push-pull (charge/discharge) electrical circuit based on semiconductor switches, similar to the one described in paper (Malyushevskaya, et al., 2021; Przystupa et al., 2020).

A dielectric chamber made in the form of a parallelepiped of organic glass plates with a working cavity of 60×60×100 mm was used as a discharge reactor. In the working cavity, two lamellar iron electrodes were installed vertically on two opposite walls along their entire plane, connected to the discharge circuit of the capacitor battery through a thyristor commutator. Additional inductances of different denominations were included in the circuit as necessary. The capacity of the capacitor battery varied widely for different series of experiments. The charging voltage of the capacitor battery was changed to include a universal power supply in its charging circuit. After charging the source to the required level (maximum − 600 V), the thyristor switch was turned on by applying a control pulse to it. Thus, the capacitor battery was switched to the inter-electrode interval with a certain frequency. The inter-electrode gap was filled with a mixture of iron and aluminum granules immersed in water. The height of the granule layer was 60 mm, the studies were carried out for a mixture of metal granules (aluminum + iron, in a mass ratio of 1:1) that was effective from the point of view of

electroplating, the average characteristic size of the granule was 5 mm. Model Fluid – Tap Water (~10^{-2} $Om^{-1}·m^{-1}$). The fluid movement pattern is vertical, bottom-up, with a volumetric flow velocity of 50 dm^3/h (Przystupa et al., 2020).

The variable values of the electrical parameters of the discharge circuit and the rationale for their selection were given further in the text during the presentation of the results and their discussion.

RESULTS AND DISCUSSION

Electrical and energy characteristics of electric spark discharge between metal granules depending on the inductance of the discharge circuit for different capacitor charging voltages In this cycle of experiments, the capacitance of the capacitor battery was fixed at 40 μF, the charging voltage of the storage device (U_0) was changed from 150 to 600 V (with an interval of 50 V). An additional inductance L (a sectioned coil without a core) of the following value, μH, was sequentially introduced into the discharge circuit: 2.13; 12.77; 22.85; 34.08; 44.14; 56.46. Satisfactory reproduction from discharge to discharge of the shape and levels of discharge current and voltage dependencies on time (hereinafter referred to as stable electrical modes of processing) in the interelectrode interval was observed for the highest range inductance at $U_0 \geq 300$ V, for the lowest at $U_0 \geq 400$ V (Fig. 1).

This result is consistent with the data of the authors (Petrichenko et al., 2015) on the minimum voltage required to form an electric spark discharge on one pair of contacts when using conductive granules made of the same material. The obtained data also correspond to the method proposed in paper (Petrichenko et al., 2016) for determining the minimum stress of multi-spark discharge formation between metal granules in layers of different geometries.

Qualitative differences in electrical characteristics were found when the additional inductance L was changed at the stage of stabilization of electrical modes. For example, for L = 56.46 μH, there is a longer formation of an end-to-end spark chain for the flow of current from electrode to electrode. The closure of the interelectrode gap by a chain of sparking contacts is accompanied by a sharp decrease in the voltage drop.

For unstable electrical modes, the closure of the interelectrode gap is accompanied by a bend in the discharge current curve (Fig. 1a, U_0 = 200 V, shown by an arrow). The process continues with the gradual monotonous development of already-formed spark chains.

At L = 2.13 μH, one end-to-end spark chain is rapidly formed, but after that, new chains are re-formed during the same pulse and the first one is partially degraded. This process is represented in multiple alternating (derivative) inflections of the discharge current curve. This feature of the

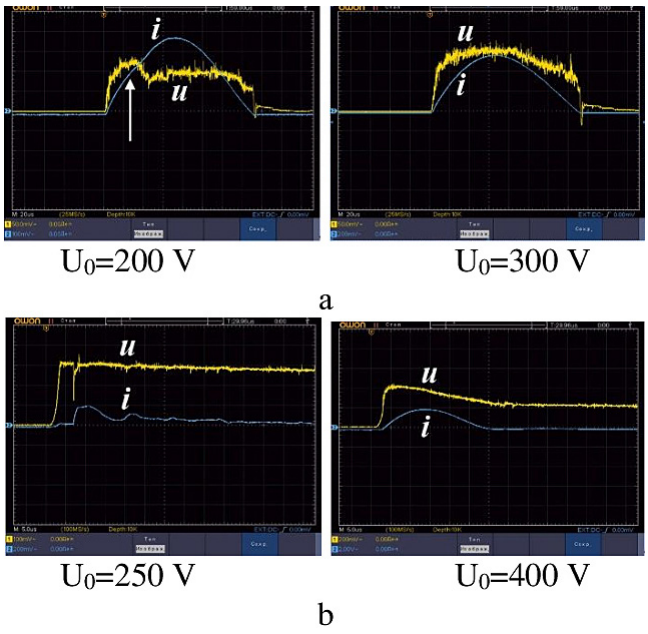

Figure 1. Stabilization of electrical processing modes: oscillograms of discharge current (i) and voltage at the interelectrode gap (u) for L = 56.46 μH (a) and L = 2.13 μH (b) at different U_0

instability of the electrical processing modes is maintained for the same L when using a larger capacitor battery (Fig. 2a). Increasing the U_0 level to the stabilization values for the data L and C eliminates instability (Fig. 2b).

The use of other L values within the studied range does not lead to the appearance of additional features and does not qualitatively change the described current and voltage dependencies on time for an electric spark discharge.

In the following, the electrical processing modes that are close to stable and fully stabilized were considered. For them, with fixed C and variable L, the charging voltage of the capacitor battery was set at U_0 (300 V. As it is shown in Figure 3, there are some regularities for all instantaneous powers that develop under load depending on L for different U_0. Instantaneous powers are calculated based on of oscillograms from the formula 1:

$$N(t) = i(t) \cdot u(t), [B \cdot A] \quad (1)$$

where: is $i(t)$ and $u(t)$ – time dependencies of discharge current and voltage at the interelectrode interval.

The maximum values of $N(t)$ for all combinations of the parameters under study, which provide stable discharges, correspond to the post-switching moment in time (formula 2)

$$\tau_{Nm} = \tau_{HP}/2.5 \quad (2)$$

where: $\tau_{HP} = \pi\sqrt{L \cdot C}$ – half-life of natural oscillations of a given discharge circuit.

Secondly, the amplitudes of the instantaneous spark discharge powers (Nm) for the same U_0 vary in inverse proportion to $L^{1/2}$. The only exception is the experiment with U_0 = 300 V for L = 2.13 μH; however, it has been shown above that this combination of parameters does not yet provide stable stabilization of the electrical processing modes. The described regularity of the dependence of the amplitude of instantaneous power on inductance is confirmed by the results of regression analysis (Nim) of the dependencies of Nm on L for different values of U_0 (Fig. 4). When analyzing the formal notation of the power regression of the instantaneous power amplitudes $N_{im}(L)$, which is defined for L in dimension [μH] (3), it turns out that the ratio of the coefficients before L for different charging voltages is close to the square ratios of the stresses themselves, and the negative exponents at L increase monotonically. The power regression was obtained using the Serpik Graphs v1.21 software package.

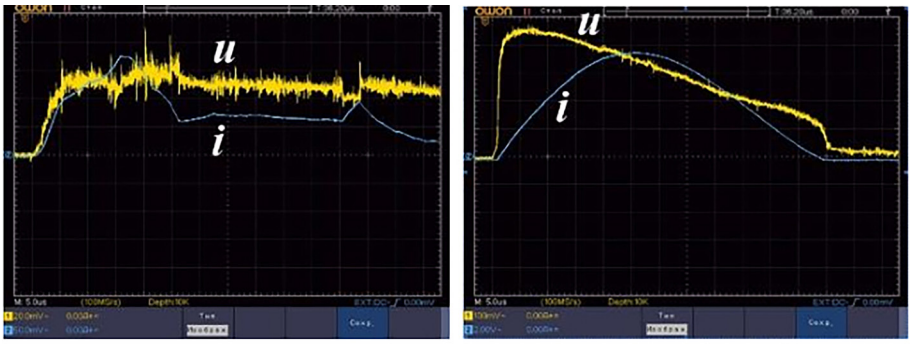

Figure 2. Oscillograms of a tightened spark process with a two-peak discharge current (a), and a stable electric discharge in a layer of granules (b) at the same values of L and C (time sweeps are the same)

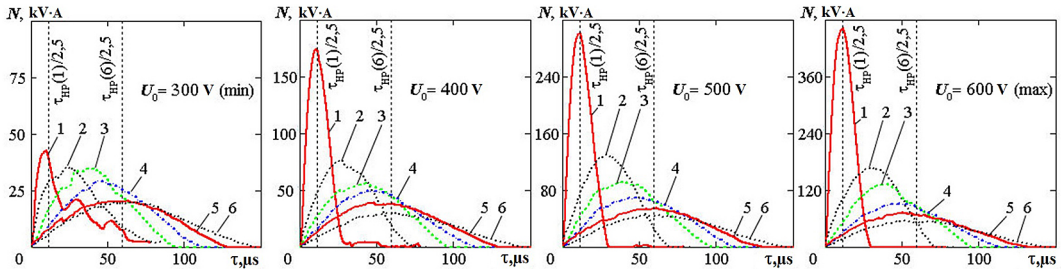

Figure 3. Experimental dependencies of instantaneous spark discharge powers: 1 – L = 2.13 μH; 2 – L = 12.77 μH; 3 – L = 22.85 μH; 4 – L = 34.08 μH; 5 – L = 44.14 μH; 6 – L = 56.46 μH

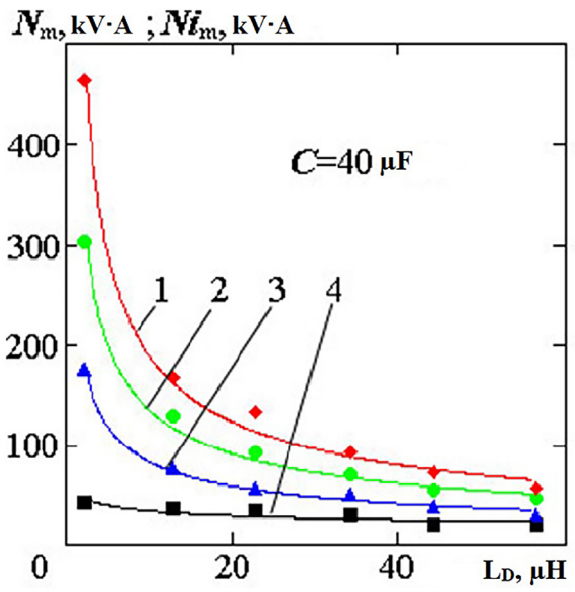

Figure 4. Experimental values (markers, *Nm*) and regression dependencies (solid lines, N_{im}) of the power amplitudes of the electric spark discharge: 1 – U_0 = 600 V; 2 – U_0 = 500 V; 3 – U_0 = 400 V; 4 – U_0 = 300 V

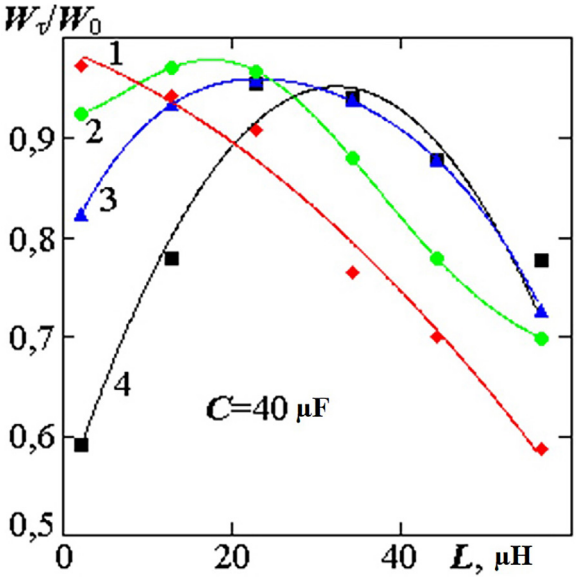

Figure 5. Dependencies of the relative energy efficiency of an electric spark discharge when varying the inductance of a discharge circuit, 1 – U_0 = 600 V; 2 – U_0 = 500 V; 3 – U_0 = 400 V; 4 – U_0 = 300 V

$$Ni_m(L) = \begin{cases} 117027 \cdot L^{-0,43}, & U_0 = 300\ V \\ 266725 \cdot L^{-0,51}, & U_0 = 400\ V \\ 497542 \cdot L^{-0,57}, & U_0 = 500\ V \\ 785539 \cdot L^{-0,62}, & U_0 = 600\ V \end{cases} \quad (3)$$

$$Na_m(U_0, C, L) = \frac{U_0^2}{\sqrt{\frac{L}{C}}} \cdot e^{-\frac{\pi}{2,5}} \quad (4)$$

It is impossible to take L beyond the lower limit of the studied range in real installations due to technical limitations, and it is impractical to increase it beyond the upper limit due to sharply increasing losses in the discharge circuit.

Thus, taking into account the moment in time, which corresponds to the maximum instantaneous power for all the investigated inductances (2), with the basic realization of an electric spark discharge in a liquid, it is possible to propose expression (4) for estimating the values of Nm as a function of U_0, C, and L (Fig. 5).

The estimation was performed at C = const = 40 μF, but as it was shown below, this expression is also valid when C changes in the parameter ranges under consideration. An accurate estimation of the instantaneous power will also require taking into account the geometric characteristics of the granule layer, the choice of which is justified in the paper (Petrichenko et al., 2016). Therefore, expression (4) is an approximation dependence of the discharge power amplitudes on the basic parameters of the discharge circuit.

The relative deviations (δ_{Nm}) of the *Nam* values calculated on the formula (4) from the corresponding experimental data *Nm* were determined by the formula 5:

$$\delta_{Nm} = \frac{\left|Na_m(U_0, C, L) - N_m(U_0, C, L)\right|}{N_m(U_0, C, L)} \cdot 100\% \quad (5)$$

and correlated with the values of the relative energy efficiency of the discharge (η_W)

$$\eta_W = W_\tau / W_0 = \frac{\int_0^{\tau 1} i(t) \cdot u(t) dt}{CU_0^2 / 2} \quad (6)$$

where: W_τ – energy released in the interelectrode gap during a discharge of τ_1, J; W_0 – energy stored before discharge in a capacitor battery, J.

According to the accepted practice of electric discharge technologies, a relative energy efficiency value of more than 0.85 is appropriate for industrial applications. The comparison (Table 1) showed that for modes with relative energy efficiency of more than 0.85, the relative deviation of the maximum power values is several percent (the maximum is 10.3%). Thus, to obtain the maximum efficient use of electrical energy in the course of electric spark treatment, expression (4) can be used as a complex

Table 1. Relative deviations of design power amplitudes and relative energy efficiency in the course of an electric spark discharge with a change in the inductance of the discharge circuit

L, μH	δ_{Nm}, %	η_W	δ_{Nm}, %	η_W	δ_{Nm}, %	η_W	δ_{Nm}, %	η_W
	U_0 = 600 V		U_0 = 500 V		U_0 = 400 V		U_0 = 300 V	
2.1	4.2	0.96	2.1	0.91	12.7	0.83	–	0.57
12.8	8.4	0.93	3.1	0.96	6.6	0.92	28.1	0.77
22.9	1.5	0.90	2.4	0.95	6.5	0.95	3.2	0.92
34.1	20.3	0.75	10.1	0.87	1.5	0.95	6.4	0.94
44.1	33.5	0.72	22.4	0.77	10.3	0.87	7.7	0.87
56.5	53.0	0.60	31.7	0.68	26.4	0.83	18.0	0.85

dependence of the electrical characteristics of the electric spark discharge in a liquid on the parameters of the discharge circuit at a fixed capacitance C. The dependencies of relative energy efficiency on inductance (Fig. 6) are extreme (except for Graph 1 in Figure 5, for which the extremum lies in the range of L values less than the lower limit of the studied range). The values of L, at which the maximum relative energy efficiency for each U_0 is observed, are the conditions for matching the spark load in the discharge circuit with a capacitor battery of a certain capacity C. These are also the conditions for optimizing the parameters of the discharge circuit of electrical installations with technological action based on electric spark treatment to minimize unproductive energy consumption.

Electrical and energy characteristics of electric spark discharge between metal granules depend on the capacitance of the discharge circuit for different charging voltages

As it was shown above, large instantaneous powers of the electric spark discharge are observed at small values of the inductances of the discharge circuit (Fig. 3, Graph 1).

Increasing the instantaneous power reduces the probability of the well-known "metal loading pellet welding" effect and contributes to the "bridge cutting" effect between pellets that have already undergone the welding effect. At present, in electrical installations using electric spark discharge, most electrical equipment designers try to reduce even the naturally formed inductance of the discharge circuit. This is dictated by considerations of increasing the maximum electrical power in the spark load. The inductance of the discharge circuit of a typical electrical installation with its optimal topology, without the use of additional means of reduction, is 2 ± 1 μH Therefore, for further studies, an L value of ≈ 2.15 μH was selected and recorded. This value varied slightly in the range from 2.1 to 2.2 μH due to natural reasons related to the arrangement of capacitors in the capacitor battery to gain the required capacity of the energy storage device and the difference in the intrinsic inductances of the capacitors. The dependencies of the electrical and energy characteristics of electric spark discharges between

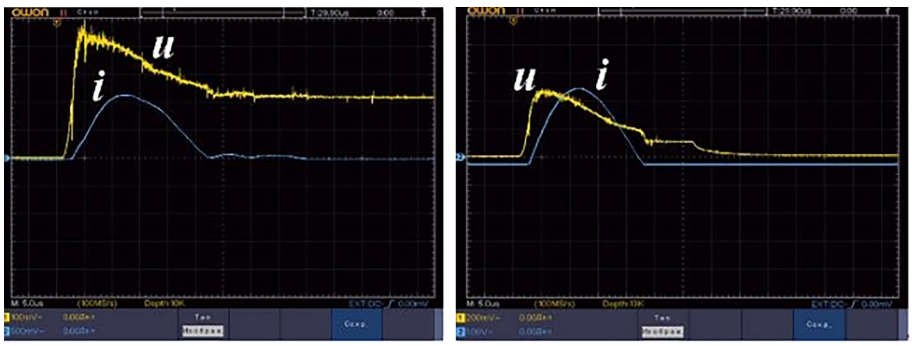

Figure 6. Oscillograms of discharge current and voltage at the interelectrode gap for C = 20 μF

granules in a liquid on the following capacitance of the capacitor battery, μF: 20; 40; 70; 100. The charging voltage of the capacitive energy storage device varied from 300 to 600 V (with an interval of 50 V), lower values of U_0 were not used due to the impossibility of stabilizing the electrical modes (as shown above). The experiments were carried out under the same conditions as for the determination of the dependence of the characteristics on L.

It was established that for C = 20 μF the discharge is formed already at U_0 = 300 V, but the forms and levels of time dependencies of the discharge current and voltage at the interelectrode interval are not reproduced from discharge to discharge even at U_0 = 400 V (Fig. 6 a). Stabilization of the electrical modes of the electric spark discharge in the circuit with C = 20 μF is observed under the condition of $U_0 \geq$ 500 V (Fig. 6b). For other capacitors of the capacitor battery, the stabilization of electrical modes occurs:

- for C = 40 μF – with condition $U_0 \geq$ 400 V;
- for C = 70 μF – with condition $U_0 \geq$ 400 V;
- for C = 100 μF – with condition $U_0 \geq$ 300 V.

When U_0 is increased to the values corresponding to the beginning of stabilization of electrical processing modes.

Thus, as the capacitance of the capacitor battery increases, the charging voltage required to stabilize the electrical modes of the electric spark discharge decreases when the shapes and amplitudes of the discharge currents and discharge voltages in the charge-discharge cycle of the capacitor battery are repeated. If the discharge current has several ripples, this usually indicates that the reproduction of the pulsed parameters of the discharge will not be observed, and the energy loss will be significant, from 20 to 70%.

The assumption was confirmed that the amplitudes of instantaneous power in the spark load for all capacitances of the studied range (Fig. 7, boundary variants from the capacitance range are shown) at fixed L correspond to the time point $\tau_{Nm} = \tau_{HP}/2.5$, as it was for all L at fixed C (Fig. 3). This makes it possible to use Formula 4 under conditions of variation C over a wide range. For all stable spark discharges in the layer of metal granules, the relative deviation from the experimental data calculated based on (4) power amplitude (Fig. 8a, solid lines) does not exceed a few percent (Table 2). At the same time, such discharges are characterized by relative energy efficiency $\eta_W > 0.85$ (Fig. 8, Table 2).

On the basis of the results obtained, the approach proposed in the paper (Petrichenko et al., 2016), where the authors presented unified time dependencies of changes in the electric power of an underwater electric discharge in the form of a triangle: equilateral – for short-term $\tau_{HP} \leq (30 \div 40)$ μs and non-equilateral – for long-term $\tau_{HP} > 40$ μs.

The difference lies in the fact that for an underwater electric spark discharge between metal granules (including in a mixture of iron and aluminum granules), the separation by the duration of the discharge can be omitted and the time dependence of electric power on time can be represented in the form of a triangle with a vertex that falls on the moment $\tau_{Nm} = \tau_{HP}/2{,}5$, according to Equation 7:

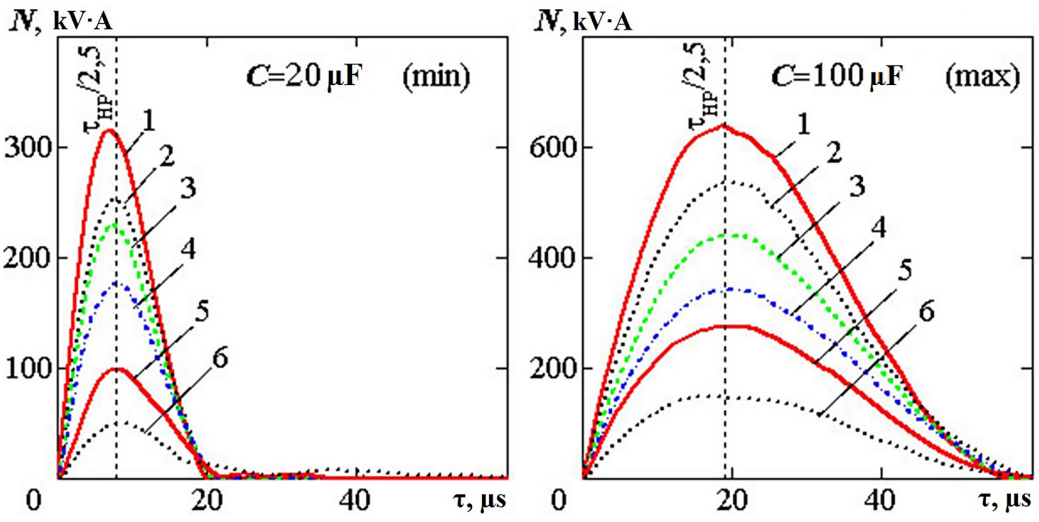

Figure 7. Experimental dependencies of instantaneous spark discharge powers: 1 – U_0 = 600 V; 2 – U_0 = 550 V; 3 – U_0 = 500 V; 4 – U_0 = 450 V; 5 – U_0 = 400 V; 6 – U_0 = 300 V.

Table 2. Relative deviations of design power amplitudes and relative energy efficiency in the course of electric spark discharge when changing the capacitor battery of the discharge circuit

C, μF	d_{Nm}, %	h_W	d_{Nm}, %	h_W	d_{Nm}, %	h_W	d_{Nm}, %	h_W
	U_0 = 300 V		U_0 = 400 V		U_0 = 500 V		U_0 = 600 V	
20	–	0.765	–	0.780	5.9	0.850	1.0	0.853
40	–	0.590	12.8	0.820	2.2	0.920	4.1	0.970
70	–	0.370	14.7	0.779	8.6	0.980	9.1	0.976
100	12.3	0.970	7.5	0.980	6.4	0.987	6.7	0.952

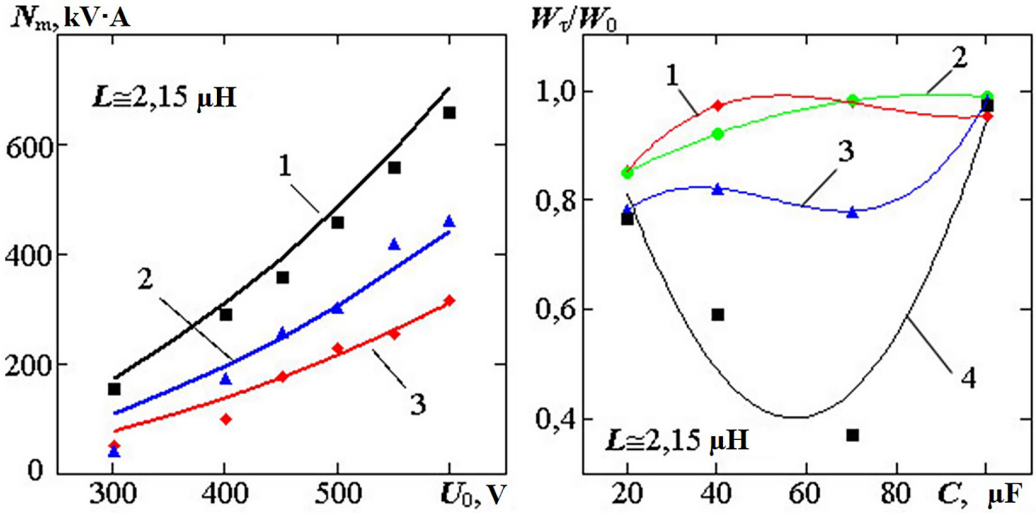

Figure 8. Dependencies (4) and experimental values of the power amplitudes of the spark discharge (a) and its relative energy efficiency when varying the capacitance (b)

$$N_{Da}(t) \approx \begin{cases} 2{,}5 \cdot \dfrac{U_0^{\,2}}{\sqrt{L/C}} \cdot e^{-\frac{\pi}{2{,}5}} \cdot \dfrac{t}{\tau_{HP}}, & 0 \le \dfrac{t}{\tau_{HP}} \le \dfrac{1}{2{,}5} \\ \dfrac{2{,}5}{1{,}5} \cdot \dfrac{U_0^{\,2}}{\sqrt{L/C}} e^{-\frac{\pi}{2{,}5}} \cdot \left(1 - \dfrac{t}{\tau_{HP}}\right), & \dfrac{1}{2{,}5} < \dfrac{t}{\tau_{HP}} \le 1 \\ 0, & 1 < \dfrac{t}{\tau_{HP}} \end{cases} \quad (7)$$

In this case, the regularities of the introduction of electrical energy into the inter-electrode gap during an underwater electric spark discharge can be written in the following form:

$$W_{Da}(t) \approx \begin{cases} W_{1/2,5}(t) = 1{,}25 \cdot \dfrac{U_0^{\,2}}{\sqrt{L/C}} \cdot e^{-\frac{\pi}{2{,}5}} \cdot \dfrac{t^2}{\tau_{HP}}, 0 \le \dfrac{t}{\tau_{HP}} \le \dfrac{1}{2{,}5} \\ W_{1/2,5}\left(\dfrac{\tau_{HP}}{2{,}5}\right) + \dfrac{1}{15} \cdot \dfrac{U_0^{\,2}}{\sqrt{L/C}} e^{-\frac{\pi}{2{,}5}} \times \\ \times \left(25 \cdot t - \dfrac{12{,}5}{\tau_{HP}} \cdot t^2 - 8 \cdot \tau_{HP}\right), \quad \dfrac{1}{2{,}5} < \dfrac{t}{\tau_{HP}} \le 1 \\ 0{,}9 \cdot W_0, \quad 1 < \dfrac{t}{\tau_{HP}} \end{cases} \quad (8)$$

Thus, the conditions for electric spark purification of water with losses of no more than 10% of the energy of the capacitor battery charge have been revealed.

CONCLUSIONS

The possibility of optimizing low-voltage (up to 1000 V) cleaning of galvanic wastewater from heavy metal ions by the electric spark method to achieve maximum efficiency is shown.

For a mixed metal load consisting of iron and aluminum granules, the general regularities of changes in the electrical characteristics of underwater electric spark discharges in the granule layer when varying the parameters of the discharge circuit were revealed.

The dependencies of the discharge power amplitudes on the capacitance, inductance and charging voltage in the discharge circuit were formalized, and the regularities of electrical energy input into the interelectrode gap were obtained.

The conditions and ranges of application of such dependencies, as well as the general conditions for stabilizing the electrical modes of electroplating treatment using an underwater electric spark discharge were determined. The existence of maximums of the relative energy efficiency

of the discharge between the granules in the interelectrode gap for matching the spark load was shown, and the conditions that allow limiting the losses in the discharge circuit to ten percent of the energy stored in the capacitor battery were found.

The obtained data make it possible to expand the effective use of electric spark purification of water from heavy metal ions.

REFERENCES

1. Berkowitz, A.E.; Hansen, M.F.; Parker, F.T.; Vecchio, K.S.; Spada, F.E.; Lavernia E.J.; Rodriguez R. 2003. Amorphous soft magnetic particles produced by spark erosion. Journal of Magnetism and Magnetic Materials, 1–6, 254–255. https://doi.org/10.1016/S0304-8853(02)00932-0
2. Béjar, M.A.; Schnake, W.; Saavedra, W.; Vildósola, J.P. 2006. Surface hardening of metallic alloys by electrospark deposition followed by plasma nitriding. Journal of Materials Processing Technology, 176(1–3), 210−213. https://doi.org/10.1016/j.jmatprotec.2006.03.162
3. Carrey, J.; Radousky, B.; Berkowitz, A. E. 2004. Spark-eroded particles: Influence of processing parameters. J. Appl. Phys., 3(95), 823−830. https://doi.org/10.1063/1.1635973
4. Lobanova, G.; Yurmazova, T.; Shiyan, L.; Voyno, D. 2015. Investigation of the mechanism of microplasma impact on iron and aluminum load using solutions of organic substances. IOP Conf. Series: Materials Science and Engineering, 81. http://dx.doi.org/10.1088/1757-899X/81/1/012076
5. Malyushevskaya, A.; Koszelnik, P.; Yushchishina, A.; Mitryasova, O.; Mats, A.; Gruca-Rokosz, R. 2023. Eco-Friendly Principles on the Extraction of Humic Acids Intensification from Biosubstrates. Journal of Ecological Engineering, 24(2), 317–327. https://doi.org/10.12911/22998993/156867
6. Malyushevskaya, A.; Yushchishina, A.; Mitryasova, O.; Pohrebennyk, V.; Salamon, I. 2021. Optimization of Extraction Processes of Water-Soluble Polysaccharides under the Electric Field Action. Przegląd Elektrotechniczny, R. 97(12), 73–76. http://doi:10.15199/48.2021.12.12
7. Milligan, J.; Shockley, J.M.; Chromik, R.R.; Brochu, M. 2013. Tribological performance of Al–12Si coatings created via Electrospark Deposition and Spark Plasma Sintering. Tribology International, 66, 1−11. https://doi.org/10.1016/j.triboint.2013.04.006.
8. Mitryasova O.; Pohrebennyk, V.; Kochanek, A.; Sopilnyak, I. 2016. Correlation Interaction between Electrical Conductivity and Nitrate Content in Natural Waters of Small Rivers. Conference Proceedings 16th International Multidisciplinary Scientific Geoconference SGEM 2016, Vienna, Austria, 2 November – 5 November 2016, 3(3), 357–365.
9. Mitryasova O.; Pohrebennyk, V. 2017. Integrated Environmental Assessment of the Surface Waters Pollution: Regional Aspect. Conference Proceedings 17th International Multidisciplinary Scientific GeoConference SGEM 2017, Vienna, Austria, 27 November – 29 November 2017, 33(17), 235– 242.
10. Petrichenko, S.; Kuskova, N.; Listovskij, D. 2015. Comparison of the electrical characteristics of spark discharges in a layer of metal and graphite granules immersed in liquid. Surf. Engin. Appl. Electrochem, 3(51), 240–245. https://doi.org/10.3103/S1068375515030138
11. Petrichenko, S.; Listovskij, D.; Kuskova, N. 2016. Stabilization of discharge pulses and peculiarities of matching spark load during electroerosive dispersion of metal and graphite granules in a liquid. Surf. Engin. Appl. Electrochem, 2(52), 134–139. https://doi.org/10.3103/S1068375516020101
12. Petrov, O.; Petrichenko, S.; Yushchishina, A.; Mitryasova, O.; Pohrebennyk, V. 2020. Electrospark Method in Galvanic Wastewater Treatment for Heavy Metal Removal. Applied Sciences, Special Issue Determination and Extraction of Heavy Metals from Wastewater and Other Complex Matrices, 10(15), 5148. https://doi.org/10.3390/app10155148
13. Przystupa, K.; Petrichenko, S.; Mitryasova, O., Yushchishina, A.; Pohrebennyk, V.; Kochan, O. 2020. Electric spark method of purification of galvanic waste waters. Przeglad Elektrotechniczny, 96(12), 230–233. https://doi.org/doi:10.15199/48.2020.12.50
14. Wang De; Gao, J.; Deng, Sh.; Wang, W. 2022. A novel particle planting process based on electrospark deposition. Materials Letters, 306, 130872. https://doi.org/10.1016/j.matlet.2021.130872
15. Zakharchenko, S.N.; Kondratenko, I.P.; Perekos, A.E.; Zalutsky, V.P.; Kozyrsky, V.V.; Lopatko, K.G. 2002. Influence of discharge pulses duration in a layer of iron granules on the sizes and structurally-phase condition of its electroerosion particles. Eastern-European Journal of EnterpriseTechnologies, 5(60), 66–72. https://doi.org/10.15587/1729-4061.2012.5728
16. Zakharchenko, S.; Perekos, A.; Shidlovska, N.; Ustinov, A.; Boytsov, O.; Voynash, V. 2018. Electrospark Dispersion of Metal Materials. I.Influence of Velocity of Flow of Operating Fluid on Dispersity of Powders. Metallofiz. Noveishie Tekhnol., 3(40), 339–357. https://doi.org/10.15407/mfint.40.03.0339